7-2007

A Spitzer White Dwarf Infrared Survey

F. Mullally
University of Texas at Austin

Ted von Hippel
University of Texas at Austin, vonhippt@erau.edu

et al.

The Astrophysical Journal Supplement Series, 171:206–218, 2007 July

A *SPITZER* WHITE DWARF INFRARED SURVEY

F. Mullally,[1] Mukremin Kilic,[1] William T. Reach,[2] Marc J. Kuchner,[3] Ted von Hippel,[1]
Adam Burrows,[4] and D. E. Winget[1]
Received 2006 July 1; accepted 2006 November 17

ABSTRACT

We present mid-infrared photometry of 124 white dwarf stars with the *Spitzer Space Telescope*. Objects were observed simultaneously at 4.5 and 8.0 μm with sensitivities better than 0.1 mJy. This data set can be used to test models of white dwarf atmospheres in a new wavelength regime, as well as to search for planetary companions and debris disks.

Subject headings: infrared: stars — surveys — white dwarfs

1. INTRODUCTION

White dwarf stars (WDs) are the evolutionary end point of stellar evolution for all main-sequence stars with a mass $\lesssim 8\ M_{\odot}$ (Weidemann 2000). The mass of an isolated WD is believed to be uniquely determined by the progenitor mass; hence, the progenitor lifetime for a WD can be estimated. Nuclear burning has ceased, so its evolution is one of monotonic and predictable cooling. From the mass and temperature of a WD its cooling age can be calculated. A white dwarf is a stellar gravestone with a date of birth and death carved on it.

Previous white dwarf infrared surveys have concentrated on the near-infrared. Zuckerman & Becklin (1992) surveyed 200 stars down to $K = 16$, while Farihi et al. (2005) surveyed 371 WDs (including 82 for which data came from Zuckerman & Becklin 1992) using several different telescopes. In the mid-infrared Chary et al. (1998) surveyed 11 WDs (and one subdwarf) with ISOCAM at 7 and 15 μm. Our survey significantly extends these previous works by looking at a large (124) sample of stars at 4.5 and 8.0 μm with a limiting sensitivity of better than 0.1 mJy. This data set allows us to study the behavior of white dwarf atmospheres in this wavelength range and to search for companion planets and disks. Such a large data set will also undoubtedly be useful to other researchers for unanticipated reasons.

The primary purpose of our survey was to search for the presence of planets and brown dwarf companions. With radii $\sim 1\ R_{\oplus}$, WDs are orders of magnitude less luminous than their progenitor stars. This dramatically reduces the contrast between the host star and any orbiting daughter planets. Probst (1983) reported on the first infrared search for substellar companions around WDs, while Burleigh et al. (2002) suggested using near-infrared imaging to detect $\gtrsim 3\ M_J$ planets in orbits >5 AU with 8 m telescopes. Recent attempts to directly detect a companion to a white dwarf include Debes et al. (2005, 2006) and Farihi et al. (2005). Theoretical spectra of brown dwarf stars and massive planets show a distinctive bump around 4–5 μm between absorption bands of methane and water (Sudarsky et al. 2003; Burrows et al. 2003). By comparing the observed flux in this passband with that of a nearby passband we can hope to directly detect the companion as an excess to the WD flux. Limits on planets around WDs based on this survey will be published in a later work.

Excess mid-infrared flux around a white dwarf can also be caused by a warm disk of circumstellar material. Fortunately, the spectral signature of a disk is markedly different from that of a planet or brown dwarf, showing a mostly flat continuum over a broad wavelength range. Zuckerman & Becklin (1987) discovered the first WD with an infrared excess, G29-38, and Wickramasinghe et al. (1988) first suggested that the excess was due to a circumstellar disk. Reach et al. (2005a) detected emission features of silicates at 10 μm from this disk using a *Spitzer* IRS spectrum (Houck et al. 2004).

Jura (2003) suggested that the metals in the atmosphere of G29-38 were accreted from the debris disk of a disrupted asteroid. Disks have also been detected around GD 362 (Kilic et al. 2005; Becklin et al. 2005), GD 56 (Kilic et al. 2006), and WD 2115−560 (this work). Von Hippel et al. (2006, hereafter HKK06) proposed that debris disks may be the source of the metals observed in the photospheres of approximately 25% of WDs (Zuckerman et al. 2003) and suggested that debris disks are therefore very common. Mid-infrared observations are sensitive to cooler dust at larger orbital separations and will be important in determining the origin and lifetimes of these disks.

Our survey has also uncovered some unusual behavior of the spectral energy distributions (SEDs) of cool WDs. Kilic et al. (2006) published an SED of WD 0038−226 showing a dramatic flux deficit and noted that DAs below 7000 K consistently showed a small flux deficit (although see Tremblay & Bergeron 2007). These results provide an opportunity to investigate the properties of matter in extreme conditions, but uncertainty in the infrared luminosity of the coolest WDs is an obstacle to their use in white dwarf cosmochronology to measure the age of the Galaxy.

2. TARGET SELECTION, OBSERVATIONS, AND REDUCTIONS

Drawing from the McCook & Sion Catalog (McCook & Sion 1999), we cross-referenced with the Two Micron All Sky Survey (2MASS; Skrutskie et al. 2006), selecting all stars brighter than $K_s = 15$, rejecting known binaries and planetary nebulae, for a total of 135 objects. We removed one object to avoid conflict with the Reserved Observations Catalog, and the *Spitzer* TAC removed three other WDs awarded to a different program. In total, we observed 131 objects and successfully measured the flux for 124 of these. The remaining objects were too heavily blended with other, brighter objects. A breakdown of the spectral type of each object is given in Table 1. In the course of a more detailed literature search we discovered, for a small number of stars, differences between the temperature and spectral type quoted in McCook

[1] Department of Astronomy, University of Texas at Austin, Austin, TX 78712.
[2] California Institute of Technology, Pasadena, CA 91125.
[3] NASA Goddard Space Flight Center, Greenbelt, MD 20771.
[4] Department of Astronomy and Steward Observatory, University of Arizona, Tucson, AZ 85721.

TABLE 1
CLASSIFICATIONS OF OBSERVED STARS

Type	Number
DA	98
DB	10
DC	3
DO	2
DQ	2
sd	2
Other	7

& Sion compared to more recently published values. Where applicable, references are listed in the notes to Table 2.

Each object was observed simultaneously in channels 2 and 4 (4.5 and 8.0 μm) with the IRAC camera (Fazio et al. 2004) on the *Spitzer Space Telescope* (Werner et al. 2004). Five 30 s exposures were taken of each object using a Gaussian dither pattern. The data were processed with version S11.4.0 of the IRAC pipeline, which removes well-understood instrumental signatures, to produce the basic calibration data (BCD) files.

We performed aperture photometry on these BCD files using the `astrolib` package in IDL. For most stars, we chose a 5 pixel aperture, although for a number of objects we used 2 or 3 pixels instead to avoid contaminating flux from nearby objects. We measured sky in an annulus of 10–20 pixels centered on the star. We made the appropriate aperture correction suggested by the IRAC data handbook. For channel 2 we multiplied the flux by 1.221, 1.113, and 1.050 for apertures of 2, 3, and 5, while the values for channel 4 were 1.571, 1.218, and 1.068, respectively.

The recorded flux for a stellar object is dependent on the location on the array where it was observed. This is because of both a variation in pixel solid angle (due to distortion) and a variation of the spectral response (due to varying filter response with incidence angle over the wide field of view). We accounted for these effects by multiplying the measured flux by the appropriate location-dependent correction factor as described in Reach et al. (2005b). We do not apply a correction to our photometry to account for variation in the flux as a function of location of the stellar centroid within the pixel, as this correction only applies to data taken in channel 1.

Because the sensitivity of the IRAC sensors is wavelength dependent, the recorded flux differs from the true flux in a manner that depends on the source's spectral shape. Fortunately this effect is small (of the order of the systematic uncertainty) and, as a white dwarf spectrum is dominated by a Rayleigh-Jeans tail in the mid-infrared, easily corrected. We used the values suggested in Reach et al. (2005b) of 1.011 at 4.5 μm and 1.034 at 8 μm. We did not apply color correction to objects whose SEDs were inconsistent with a single blackbody source (see Table 2). The IRAC pipeline removes some but not all cosmic rays. To clean our data of remaining artifacts, we removed frames where the flux deviated by more than 3.5 σ from the median and calculated the weighted average flux of the remaining frames.

3. RESULTS

We present the fluxes for each white dwarf in the two IRAC bands in Table 2. For comparison, we also list the flux for each object in *J*, *H*, and *K* as measured by the 2MASS survey. An SED for each object, with optical photometry from the McCook & Sion catalog, is presented in Figure 1. A blackbody at the quoted temperature and fit to the optical and near-infrared data is also shown to guide the eye. A subset of objects in this sample have been previously published in Reach et al. (2005a) and Kilic et al. (2006); we present photometry for these stars here for completeness. Note that, as these papers used an earlier version of the IRAC pipeline, their published fluxes differ slightly from those presented here.

3.1. *Notes on Individual Objects*

WD 0002+729.—A handful of stars show a small excess at 8 μm; we discuss this star as an example object. The atmosphere of WD 0002+729 is contaminated with small amounts of metals (Wolff et al. 2002), which may increase the probability of the existence of a disk. However, the flux is close to our sensitivity limits ($\approx$0.1 mJy) and our error bar may be underestimated; our confidence in this excess is low. By fitting models to this excess we can determine that if this excess is due to a disk, its maximum temperature must be less than about 300 K.

WD 0031−274.—McCook & Sion incorrectly classified this object as a DA. Kilkenny et al. (1988) classified it to be an sdOB star with their criterion "dominated by He I and He II lines; often Balmer absorption present." Lisker et al. (2005) measure a temperature of 36,097 K and a distance of 900 pc. They refer to it as an sdB. Our photometry shows a clear excess from *J* onward relative to the visible photometry. Close examination of the images does not reveal any irregularities in the point response function. At this distance, the flux from a substellar companion would be negligible. We fail to find a good fit for a low-mass main-sequence star, nor does the excess show the broad flat shape of a circumstellar dust spectrum. The excess is best fit with a blackbody temperature of 18,300 K; however, a circumstellar object of this temperature would be detectable in the visible flux. Cyclotron emission has been suggested as a source of infrared emission in WDs, but this object is not known to have a strong magnetic field. Further study is necessary to determine the true nature of this object.

WD 0038−226.—See Kilic et al. (2006) for a further discussion of this object's dramatic flux deficit.

WD 0447+176.—McCook & Sion incorrectly quote Wegner & Swanson (1990) giving a *V* magnitude of 13.4 instead of 12.65. Kilkenny et al. (1988) report $V = 12.62$ and a temperature of 33.8 kk. This temperature does not fit the SED well, and we instead plot the best-fit blackbody temperature of 15.5 kK.

WD 0843+358.—This object partially resolves into two objects separated by 2.2 pixels at 8 μm, causing the observed excess at that band. The companion object is not seen at any bluer wavelengths. Were the companion substellar in nature the excess would be greater at 4.5 μm than at 8; we therefore conclude that the excess is due to a background object. Examination of POSS 1 plates from 1953 shows no evidence of an object at the current position of the WD.

WD 1036+433.—Also known as Feige 34. Thejll et al. (1991) determine it to be an 80 kK sdO. Maxted et al. (2000) note that they observed Hα in emission from this object but the emission is intermittent, as other observers make no mention of it (Oke 1990; Bohlin et al. 2001). Chu et al. (2001), who also observe emission, suggest that this emission could be caused by photoionization of the atmosphere of a hot Jupiter companion.

Our photometry shows a clear excess from *H* onward. Examination of the individual images shows that the white dwarf is the brightest object in the vicinity, and there is no evidence of a line-of-sight companion. This excess was first observed in *J*, *H*, and *K* by Probst (1983). Thejll et al. (1991) summarized the available photometry at that time and concluded that the colors were "marginally consistent" with a companion K7–M0 dwarf. We find that the excess is well fit in color and magnitude by a 3750 K

TABLE 2

INFRARED FLUXES FOR STARS IN THIS SAMPLE

Name	Type	$T_{\rm eff}$ (K)	J (mJy)	H (mJy)	K (mJy)	IRAC 2 (mJy)	IRAC 4 (mJy)	Ap. (pixel)	Notes
WD 0002+729	DBZ	13750	2.272 (40)	1.484 (29)	0.833 (16)	0.2277 (79)	0.116 (16)	3	1
WD 0004+330	DA	47219	2.503 (44)	1.416 (28)	0.857 (16)	0.2212 (86)	0.064 (21)	5	
WD 0005+511	DO	47083	4.200 (73)	2.271 (44)	1.411 (27)	0.2975 (99)	0.096 (14)	3	
WD 0009+501	DAP	6540	6.41 (11)	5.14 (10)	3.528 (67)	1.006 (31)	0.343 (23)	5	2
WD 0018−267	DA	5275	15.88 (28)	14.72 (29)	10.51 (20)	2.923 (88)	1.134 (42)	5	
WD 0031−274	sdB	36097	2.816 (49)	1.937 (38)	1.124 (21)	0.2634 (89)	0.138 (16)	3	3
WD 0038−226	C_2H	5400	7.34 (13)	4.141 (81)	2.132 (40)	0.507 (16)	0.229 (23)	5	2, 4
WD 0047−524	DA	18188	2.117 (37)	1.257 (25)	0.961 (18)	0.1982 (73)	0.091 (15)	3	
WD 0050−332	DA	34428	3.989 (70)	2.191 (43)	1.249 (24)	0.312 (10)	0.127 (17)	3	
WD 0100−068	DB	16114	2.742 (48)	1.710 (33)	1.102 (21)	0.256 (11)	0.100 (17)	3	
WD 0101+048	DA	8080	6.32 (11)	4.486 (88)	2.862 (54)	0.792 (25)	0.315 (26)	5	
WD 0109−264	DA	31336	5.125 (89)	2.899 (57)	1.835 (35)	0.422 (14)	0.168 (22)	5	
WD 0115+159	DC	9800	5.149 (90)	3.454 (68)	2.155 (41)	0.594 (19)	0.197 (22)	3	
WD 0126+101	DA	8500	3.888 (68)	2.688 (52)	1.731 (33)	0.472 (15)	0.194 (20)	3	
WD 0126−532	DA	15131	1.828 (32)	1.122 (22)	0.710 (13)	0.1801 (66)	0.057 (14)	3	
WD 0133−116.....	DAV	10850	2.816 (49)	1.937 (38)	1.124 (21)	0.303 (10)	0.107 (16)	3	
WD 0134+833	DA	19990	5.88 (10)	3.058 (60)	2.212 (42)	0.576 (19)	0.205 (21)	5	
WD 0141−675	DA	6317	11.37 (20)	8.85 (17)	6.20 (12)	1.722 (52)	0.658 (29)	5	5
WD 0148+467	DA	13879	12.45 (22)	7.58 (15)	4.848 (92)	1.257 (39)	0.444 (29)	5	
WD 0227+050	DA	19907	7.76 (14)	4.608 (90)	2.844 (54)	0.764 (24)	0.297 (27)	5	
WD 0231−054	DA	13105	2.435 (42)	1.539 (30)	0.913 (17)	0.2249 (87)	0.086 (27)	5	
WD 0255−705	DA	10430	3.873 (68)	2.292 (45)	1.695 (32)	0.412 (13)	0.174 (16)	3	6
WD 0308−565	DB	24000	2.308 (40)	1.286 (25)	0.787 (15)	0.2243 (80)	0.093 (14)	3	
WD 0310−688	DA	15155	31.57 (55)	19.69 (38)	12.01 (23)	3.030 (92)	1.142 (41)	5	
WD 0316+345	DA	14735	2.375 (41)	1.381 (27)	0.993 (19)	0.2234 (80)	0.079 (18)	3	
WD 0407+179	DA	12268	2.709 (47)	1.610 (31)	1.097 (21)	0.280 (10)	0.110 (31)	5	
WD 0410+117	DA	18558	2.941 (51)	1.577 (31)	1.115 (21)	0.2626 (97)	0.112 (32)	5	
WD 0431+126	DA	19752	1.972 (34)	1.227 (24)	0.801 (15)	0.1815 (76)	0.044 (34)	5	
WD 0438+108	DA	25892	2.522 (44)	1.448 (28)	0.962 (18)	0.2143 (76)	0.089 (20)	3	
WD 0446−789	DA	24406	4.135 (72)	2.173 (42)	1.252 (24)	0.350 (12)	0.156 (14)	3	
WD 0447+176	DB	15500	12.71 (22)	7.43 (14)	4.764 (90)	1.135 (35)	0.415 (24)	3	
WD 0455−282	DA	57273	2.134 (37)	1.181 (23)	0.863 (16)	0.857 (27)	0.223 (26)	5	7
WD 0501+527	DA	40588	15.32 (27)	8.76 (17)	5.228 (99)	1.327 (41)	0.454 (32)	5	
WD 0503+147	DB	17714	2.614 (46)	1.569 (31)	0.966 (18)	0.2247 (77)	0.099 (17)	2	
WD 0507+045	DA	17974	2.180 (38)	1.167 (23)	0.714 (14)	0.2213 (76)	0.236 (20)	2	7
WD 0549+158	DA	34735	5.144 (90)	2.818 (55)	1.506 (28)	0.437 (14)	0.169 (19)	2	
WD 0552−041	DZ	5060	9.63 (17)	7.35 (14)	5.166 (98)	1.892 (58)	0.799 (34)	5	
WD 0553+053	DAP	5790	10.73 (19)	8.36 (16)	5.79 (11)	1.717 (52)	0.561 (26)	3	
WD 0612+177	DA	23593	4.342 (76)	2.594 (51)	1.853 (35)	0.450 (15)	0.236 (24)	2	8, 5
WD 0621−376	DA	48333	11.56 (20)	6.68 (13)	3.879 (73)	0.922 (29)	0.370 (23)	5	
WD 0644+375	DA	20950	13.79 (24)	8.82 (17)	5.271 (100)	1.350 (42)	0.487 (30)	5	
WD 0713+584	DA	10838	31.14 (54)	20.75 (40)	13.66 (26)	3.71 (11)	1.461 (50)	5	
WD 0715−703	DA	43870	2.055 (36)	1.095 (21)	0.683 (13)	0.2281 (93)	0.124 (22)	5	9
WD 0732−427	DAE	14250	2.660 (46)	1.720 (34)	1.148 (22)	0.2620 (92)	0.098 (25)	3	
WD 0752−676	DZ	5730	12.94 (23)	10.47 (20)	7.57 (14)	2.219 (67)	0.859 (30)	3	2
WD 0806−661	DQ	14633	5.259 (92)	3.271 (64)	2.049 (39)	0.519 (16)	0.209 (17)	3	10
WD 0839−327	DA	8930	37.26 (65)	24.81 (48)	16.04 (30)	4.20 (13)	1.598 (52)	3	
WD 0843+358	DZ	17103	2.144 (37)	1.442 (28)	0.971 (18)	0.2704 (100)	0.161 (24)	5	7
WD 0912+536	DCP	7160	7.57 (13)	5.32 (10)	3.722 (70)	1.150 (35)	0.454 (25)	5	
WD 1031−114.....	DA	25714	5.94 (10)	3.406 (66)	1.953 (37)	0.482 (16)	0.188 (26)	5	
WD 1036+433	sdO	80000	35.10 (61)	24.27 (47)	16.14 (30)	4.37 (13)	1.723 (57)	5	4, 11
WD 1053−550	DA	12099	2.702 (47)	1.621 (32)	1.129 (21)	0.2666 (93)	0.106 (15)	3	
WD 1055−072	DC	7420	4.949 (86)	3.454 (68)	2.691 (51)	0.674 (21)	0.289 (23)	3	2
WD 1105−048.....	DA	16051	6.93 (12)	4.288 (84)	2.549 (48)	0.655 (21)	0.266 (30)	5	
WD 1121+216	DA	7490	5.93 (10)	4.388 (86)	2.913 (55)	1.660 (51)	0.709 (27)	2	7, 5
WD 1134+300	DA	20370	10.12 (18)	5.87 (12)	3.554 (67)	0.873 (27)	0.291 (30)	5	5
WD 1202−232	DAZ	8567	17.45 (30)	12.30 (24)	7.71 (15)	2.038 (62)	0.753 (31)	3	
WD 1223−659	DA	7276	7.39 (13)	5.099 (100)	3.200 (60)	0.953 (30)	0.394 (18)	2	5
WD 1234+481	DA	55040	1.628 (28)	1.067 (21)	0.707 (13)	0.2116 (75)	0.085 (15)	3	4, 12
WD 1236−495	DAV	11550	4.787 (84)	3.050 (60)	1.824 (34)	0.468 (15)	0.167 (15)	3	
WD 1254+223	DA	40588	3.960 (69)	2.122 (41)	1.261 (24)	0.310 (10)	0.123 (18)	3	5
WD 1327−083	DA	13875	14.26 (25)	8.70 (17)	5.37 (10)	1.386 (42)	0.488 (26)	3	5
WD 1337+705	DAZ	20970	8.00 (14)	4.651 (91)	2.777 (52)	0.753 (24)	0.296 (22)	5	
WD 1407−475	DA	18892	2.022 (35)	1.208 (24)	0.728 (14)	0.2093 (77)	0.082 (17)	2	

TABLE 2—*Continued*

Name	Type	$T_{\rm eff}$ (K)	J (mJy)	H (mJy)	K (mJy)	IRAC 2 (mJy)	IRAC 4 (mJy)	Ap. (pixel)	Notes
WD 1408+323	DA	16465	2.780 (48)	1.647 (32)	1.126 (21)	0.293 (10)	0.121 (21)	5	5
WD 1425−811.....	DA	12000	5.91 (10)	3.708 (72)	2.322 (44)	0.594 (20)	0.234 (21)	5	
WD 1509+322	DA	14371	2.680 (47)	1.516 (30)	0.989 (19)	0.2640 (89)	0.108 (14)	3	
WD 1531−022	DA	18110	2.783 (48)	1.647 (32)	0.948 (18)	0.2487 (85)	0.106 (17)	3	
WD 1559+369	DAV	10286	2.705 (47)	1.916 (37)	1.169 (22)	0.2680 (89)	0.112 (13)	2	9
WD 1606+422	DA	11320	4.063 (71)	2.511 (49)	1.599 (30)	0.409 (13)	0.165 (13)	2	
WD 1611−084.....	DA	33214	2.258 (39)	1.192 (23)	0.745 (14)	0.1903 (79)	0.096 (29)	5	9
WD 1615−154	DA	29623	3.863 (67)	2.120 (41)	1.249 (24)	0.319 (11)	0.099 (18)	3	
WD 1616−390	DA	24007	5.446 (95)	4.901 (96)	3.489 (66)	1.117 (35)	0.319 (22)	3	4, 13
WD 1626+368	DBZ	8640	5.594 (98)	3.544 (69)	2.477 (47)	0.680 (21)	0.286 (17)	3	
WD 1631+396	DA	20540	1.835 (32)	1.150 (22)	0.737 (14)	0.1651 (61)	0.057 (15)	3	
WD 1637+335	DA	9940	2.410 (42)	1.673 (33)	1.133 (21)	0.2648 (90)	0.082 (16)	2	
WD 1645+325	DBV	24600	3.559 (62)	2.128 (42)	1.144 (22)	0.356 (12)	0.115 (21)	5	
WD 1647+591	DAV	12000	17.08 (30)	10.59 (21)	6.53 (12)	1.724 (52)	0.652 (28)	5	
WD 1655+215	DA	9180	4.447 (78)	3.047 (59)	1.900 (36)	0.518 (16)	0.163 (20)	3	
WD 1659−531	DA	14609	4.726 (82)	2.873 (56)	1.750 (33)	0.441 (15)	0.100 (17)	2	
WD 1713+332	DA	20630	1.748 (30)	1.052 (20)	0.689 (13)	0.1882 (66)	0.064 (12)	2	
WD 1716+020	DA	13470	2.298 (40)	1.573 (31)	0.998 (19)	0.296 (10)	0.110 (18)	2	
WD 1748+708	DXP	5590	13.15 (23)	9.98 (20)	6.62 (12)	1.981 (60)	0.802 (31)	5	
WD 1756+827	DA	7270	5.609 (98)	4.183 (82)	2.828 (54)	0.787 (25)	0.290 (21)	5	5
WD 1822+410	DZ	14350	2.285 (40)	1.395 (27)	0.877 (17)	0.2108 (74)	0.085 (19)	3	
WD 1840−111.....	DA	11587	3.526 (62)	2.481 (48)	1.449 (27)	0.501 (20)	0.231 (24)	2	7
WD 1900+705	DXP	12070	7.39 (13)	4.312 (84)	2.865 (54)	0.720 (23)	0.309 (23)	5	
WD 1919+145	DA	14838	7.91 (14)	4.261 (83)	2.544 (48)	0.818 (34)	0.631 (73)	2	7
WD 1935+276	DAV	12318	8.50 (15)	5.31 (10)	3.107 (59)	0.890 (28)	0.315 (20)	3	5
WD 1936+327	DA	18413	3.608 (63)	2.079 (41)	1.199 (23)	0.332 (11)	0.115 (18)	3	
WD 1942+499	DA	34086	1.136 (20)	0.737 (14)	0.565 (11)	0.1113 (50)	0.037 (13)	3	
WD 1943+163	DA	18851	2.550 (44)	1.441 (28)	0.936 (18)	0.2341 (90)	0.133 (15)	2	7
WD 1953−011.....	DAP	7920	9.43 (16)	6.29 (12)	4.153 (78)	1.259 (39)	0.505 (24)	3	7, 2
WD 2004−605	DA	26481	3.845 (67)	2.193 (43)	1.384 (26)	0.334 (12)	0.154 (24)	5	
WD 2007−303	DA	14990	14.77 (26)	8.99 (18)	5.56 (10)	1.433 (44)	0.589 (34)	5	
WD 2014−575	DA	27407	2.936 (51)	1.667 (33)	1.040 (20)	0.2314 (80)	0.095 (18)	3	
WD 2028+390	DA	31725	4.314 (75)	2.556 (50)	1.215 (23)	0.341 (12)	0.131 (77)	2	9
WD 2032+248	DA	20039	24.37 (42)	15.19 (30)	8.90 (17)	2.336 (71)	0.842 (35)	5	
WD 2034−532	DB	13076	1.532 (27)	1.490 (29)	0.915 (17)	0.2409 (95)	0.091 (26)	5	
WD 2039−202	DA	19373	11.82 (21)	6.95 (14)	4.191 (79)	1.058 (33)	0.382 (23)	3	
WD 2039−682	DA	17541	5.139 (90)	3.075 (60)	2.013 (38)	0.499 (16)	0.187 (21)	5	
WD 2046+396	DA	25296	1.792 (31)	1.781 (35)	1.161 (22)	0.358 (12)	0.150 (21)	2	7
WD 2047+372	DA	14118	7.61 (13)	4.595 (90)	2.826 (53)	0.774 (25)	0.224 (18)	2	
WD 2105−820	DAZ	10200	6.48 (11)	4.265 (83)	2.575 (49)	0.736 (23)	0.295 (28)	5	5
WD 2111+498.....	DA	34386	5.018 (87)	3.118 (61)	1.703 (32)	0.426 (14)	0.142 (26)	2	
WD 2115+339	DOV	170000	4.739 (83)	2.761 (54)	1.418 (27)	0.404 (14)	0.175 (22)	5	14
WD 2115−560.....	DAZ	9700	3.618 (63)	2.582 (50)	1.641 (31)	1.034 (32)	0.913 (35)	5	4, 15
WD 2117+539	DA	15394	13.49 (23)	7.88 (15)	4.830 (91)	1.320 (40)	0.532 (26)	3	5
WD 2126+734	DA	14341	9.21 (16)	5.55 (11)	3.610 (68)	0.963 (30)	0.377 (17)	2	5, 7
WD 2130−047	DB	17500	1.717 (30)	1.016 (20)	0.573 (11)	0.1477 (78)	0.073 (32)	5	16
WD 2134+218	DA	17814	1.909 (33)	1.006 (20)	0.729 (14)	0.1672 (75)	...	5	17
WD 2136+828	DA	16400	6.64 (12)	4.107 (80)	2.662 (50)	0.622 (20)	0.215 (20)	5	
WD 2140+207	DQ	8860	10.24 (18)	6.90 (14)	4.520 (85)	1.252 (39)	0.434 (26)	5	
WD 2148+286	DA	60240	49.26 (86)	27.23 (53)	15.90 (30)	4.22 (13)	1.599 (51)	3	
WD 2149+021	DAZ	17938	8.34 (14)	4.965 (97)	2.918 (55)	0.788 (25)	0.288 (28)	5	5
WD 2211−495.....	DA	58149	16.83 (29)	9.24 (18)	5.85 (11)	1.384 (42)	0.507 (29)	5	
WD 2216−657	DZ	12082	2.439 (42)	1.617 (32)	1.031 (20)	0.2913 (96)	0.098 (14)	3	
WD 2246+223	DA	10330	2.925 (51)	1.921 (38)	1.202 (23)	0.313 (10)	0.122 (16)	3	
WD 2316−173	DB	12918	3.417 (60)	2.151 (42)	1.324 (25)	0.316 (12)	0.138 (29)	5	
WD 2326+049	DAV	13003	8.91 (16)	6.03 (12)	5.60 (11)	8.80 (26)	8.64 (26)	5	4
WD 2329−291	DAWK	26620	2.451 (43)	1.481 (29)	0.895 (17)	0.2173 (89)	0.082 (32)	5	
WD 2331−475	DAZ	50400	3.562 (62)	2.038 (40)	1.275 (24)	0.2974 (99)	0.138 (16)	3	
WD 2333−165	DA	9789	5.83 (10)	3.344 (65)	2.181 (41)	0.558 (18)	0.207 (19)	3	
WD 2359−434	DAP	8690	14.58 (25)	10.97 (21)	7.01 (13)	1.841 (56)	0.692 (34)	5	

NOTES.—Infrared fluxes for stars in this survey. Values in parentheses are uncertainties for the two least significant digits for each measurment. "Ap." refers to the aperture size used in the photometry. Temperatures and spectral types are taken from McCook & Sion (1999) or Table 3, unless otherwise noted. *JHK* photometry taken from the 2MASS survey is presented here for convenience. Notes are as follows: (1) Also known as GD 408. Spectral type and temperature from Wolff et al. (2002). (2) Spectral type taken from Kilic et al. (2006). (3) Also GD 619. Spectral type and temperature from Kilkenny et al. (1988). (4) No color correction applied to this photometry. (5) Spectral type taken from SIMBAD. (6) Temperature from Giovannini et al. (1998). (7) Photometry of this star is contaminated by the flux from a nearby object and is not trustworthy. (8) Photometry of this object is affected by the diffraction spike of a bright foreground object. (9) Temperature from Finley et al. (1997). (10) The 8 μm photometry is slightly contaminated by background nebulosity. (11) Spectral type and temperature from Thejll et al. (1991). (12) Spectral type and temperature from Liebert et al. (2005). (13) Temperature from Sion et al. (1988). (14) Temperature from Werner et al. (1996). (15) Temperature from Koester & Wilken (2006). (16) Temperature from Oke et al. (1984). (17) Object not detected at 8 μm.

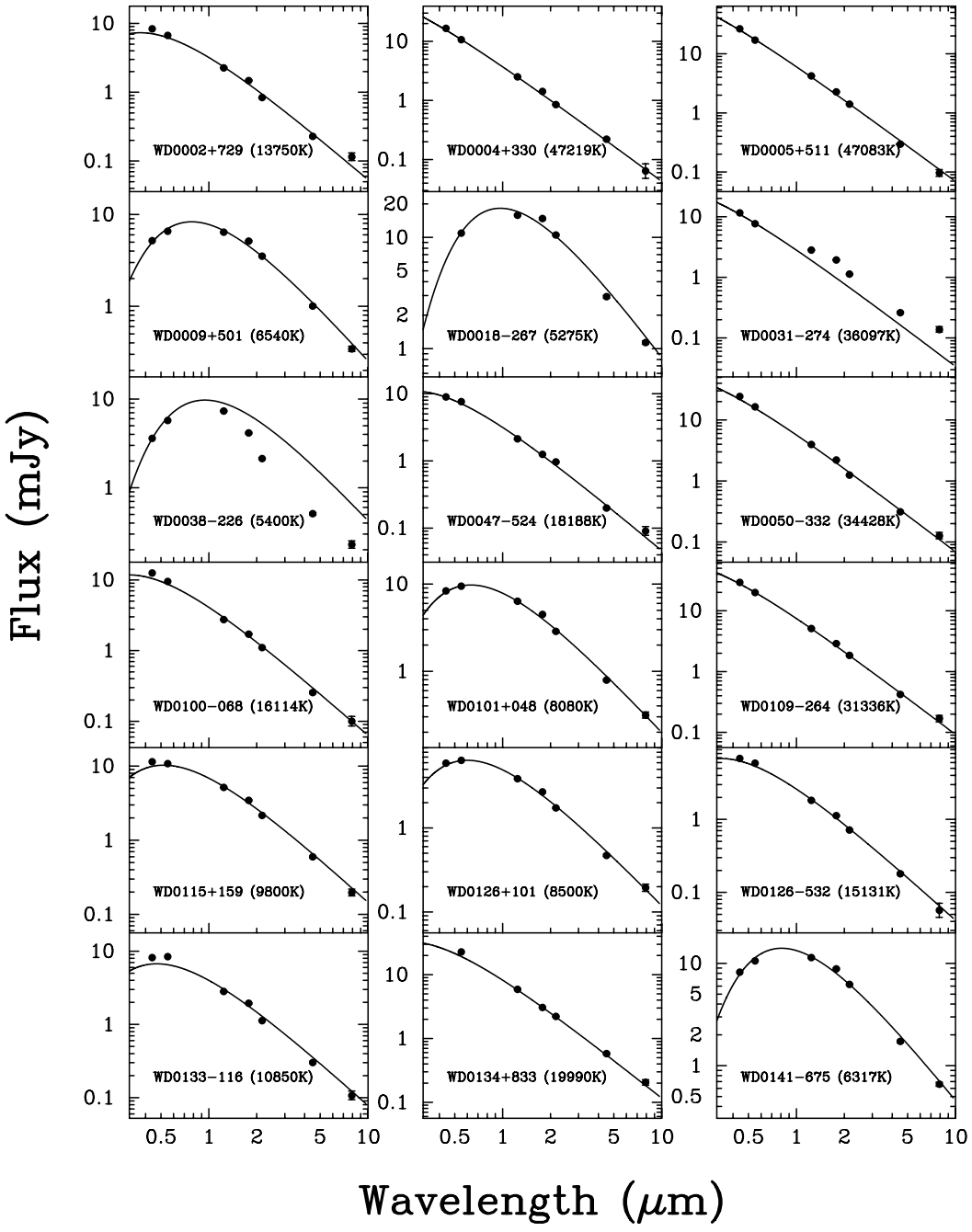

FIG. 1.—SEDs for the 124 WD stars in this survey. Our IRAC photometry points are at 4.5 and 8 μm. Also shown for comparison are near-IR fluxes from 2MASS, and *B* and *V* photometry from the McCook & Sion catalog where available. Points with arrows indicate upper limits on the flux, not measurements (see Table 2). The solid line represents a blackbody at the temperature listed in Table 2 fit to the optical and near-IR data. A blackbody is a good, but not perfect, model of a WD photosphere, and this accounts for much of the deviation in the photometry. A better fit can be achieved with atmosphere models; however, as these fits are intended only to guide the eye, a blackbody does an adequate job.

Kurucz model (Kurucz 1979), corresponding to a spectral type of M0 or M1.

WD 1234+481.—Liebert et al. (2005) measure a temperature for this star of 55,040 $\pm$ 975 K and a log g of 7.78 $\pm$ 0.06 and derive a distance of 144 pc. Holberg et al. (1998) measure 56,400 K, 7.67, and 129 pc, respectively, based on an *International Ultraviolet Explorer* spectrum. Other authors measure similar values. Debes et al. (2005) noticed an excess in the near-infrared and assigned a preliminary spectral type to the companion of M8 V.

We observe an infrared excess in all five bands. The IRAC images are round and isolated. The measured flux values in apertures of 2, 3, and 5 pixels yield consistent values, ruling out the possibility that the excess is caused by contamination from a nearby bright star. We note that the excess can be fit by a model of a brown dwarf with $T_{\rm eff} < 2000$ K corresponding to a spectral type of early L. If planned follow-up observations confirm the substellar nature of this companion, it would be the fourth white dwarf–brown dwarf binary known.

WD 1616−390.—Sion et al. (1988) list this star as a 0.61 $M_{\odot}$ DA with $T_{\rm eff}$ of 24,007 K. We notice a clear excess from *J* onward. The colors of the excess are well fit with a 4000 K Kurucz model of a main-sequence star, corresponding to a late K spectral

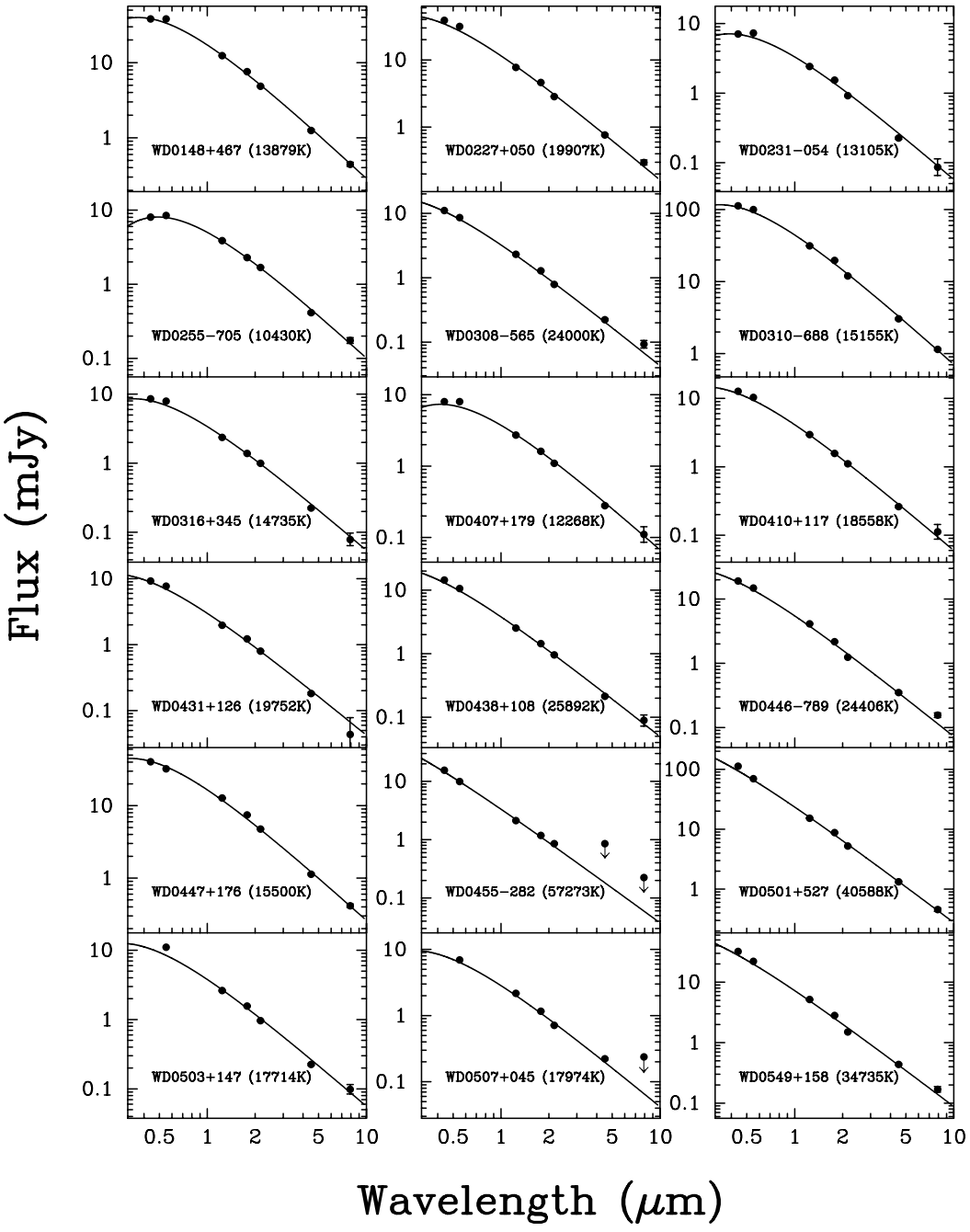

FIG. 1—*Continued*

type. However, the magnitude of the excess is too large to be consistent with a K dwarf companion. We conclude that the excess is either from a foreground dwarf star or a background giant.

WD 2115−560.—This object has an infrared excess consistent with a dust debris disk. See HKK06 for further details.

WD 2134+218.—This object was too faint to be detected at 8 μm. The expected flux according to a blackbody model was 0.05 mJy, less than our nominal detection limit of about 0.1 mJy with the 150 s exposure time used.

WD 2326+049.—This object, also known as G29-38, has an infrared excess consistent with circumstellar dust. This excess was first reported by Zuckerman & Becklin (1987). Reach et al. (2005a) fit a *Spitzer* IRS spectrum of the disk with a mixture of olivine, fosterite, and carbon dust.

4. DISCUSSION

We fit the observed SEDs of DA stars between 6 and 60 kK in the optical and near-infrared with synthetic photometry derived from models kindly supplied by D. Koester. Details of the input physics and methods are described in Finley et al. (1997), Homeier et al. (1998), and Koester et al. (2001). We then compared the observed excess (or deficit) over the fitted model in the mid-infrared to the uncertainty in the observation. Objects with disks (WD 2326, WD 2115), probable companions (e.g., WD 1234), or contaminated photometry are not included. We expect the distribution of this value for the sample to be well described by a Gaussian distribution with mean 0 and standard deviation of 1. We plot this distribution in Figure 2. The gray histogram

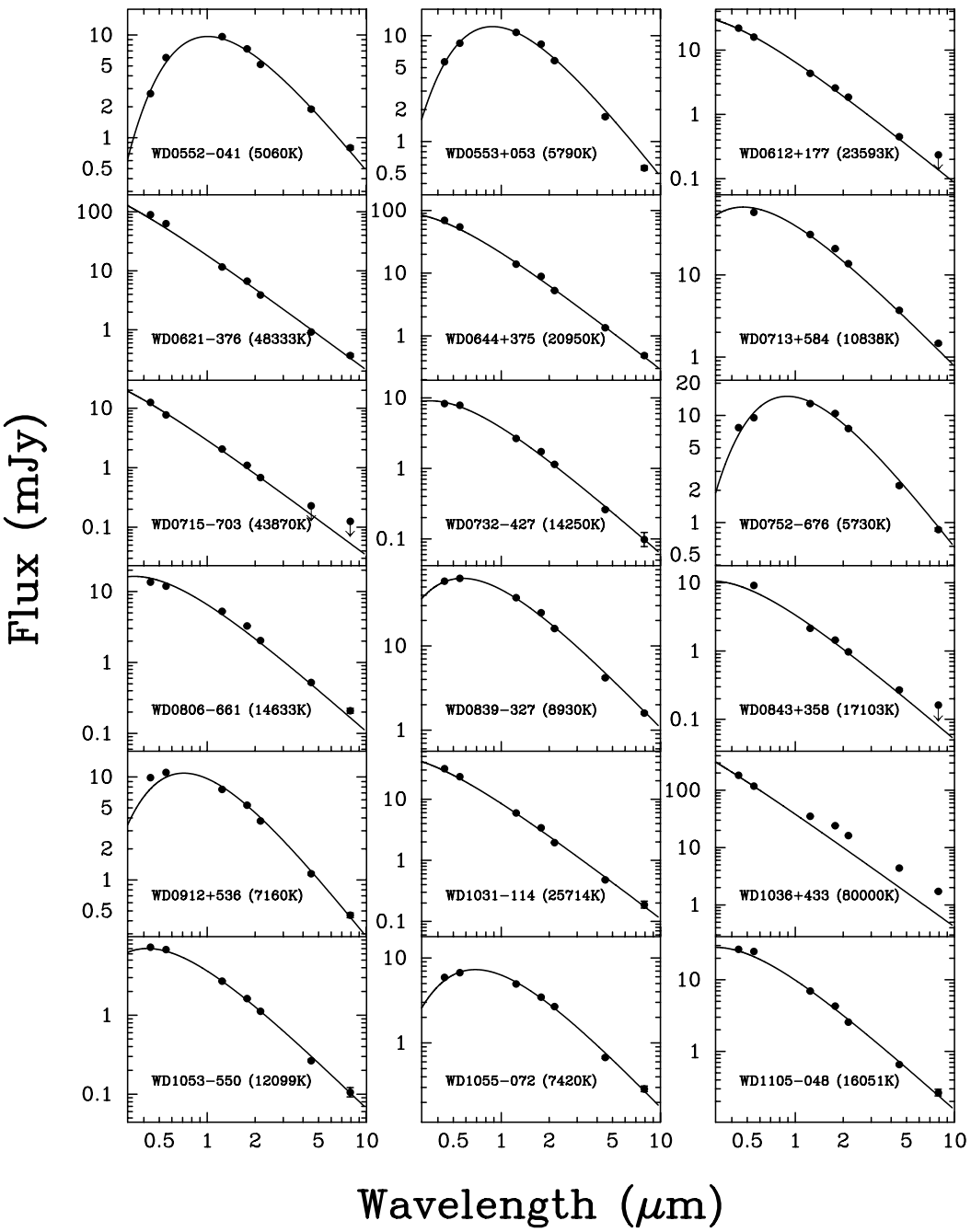

FIG. 1—*Continued*

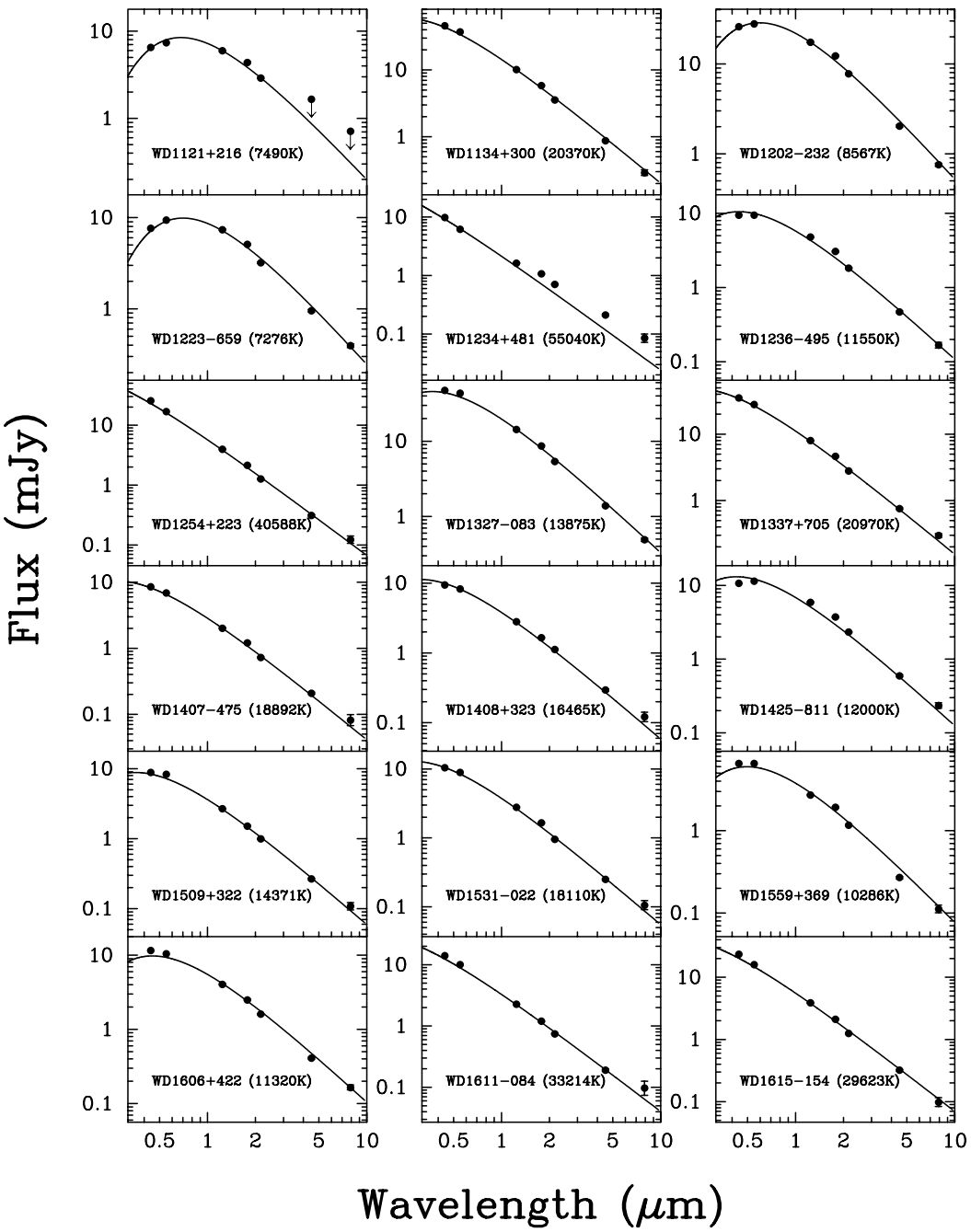

FIG. 1—*Continued*

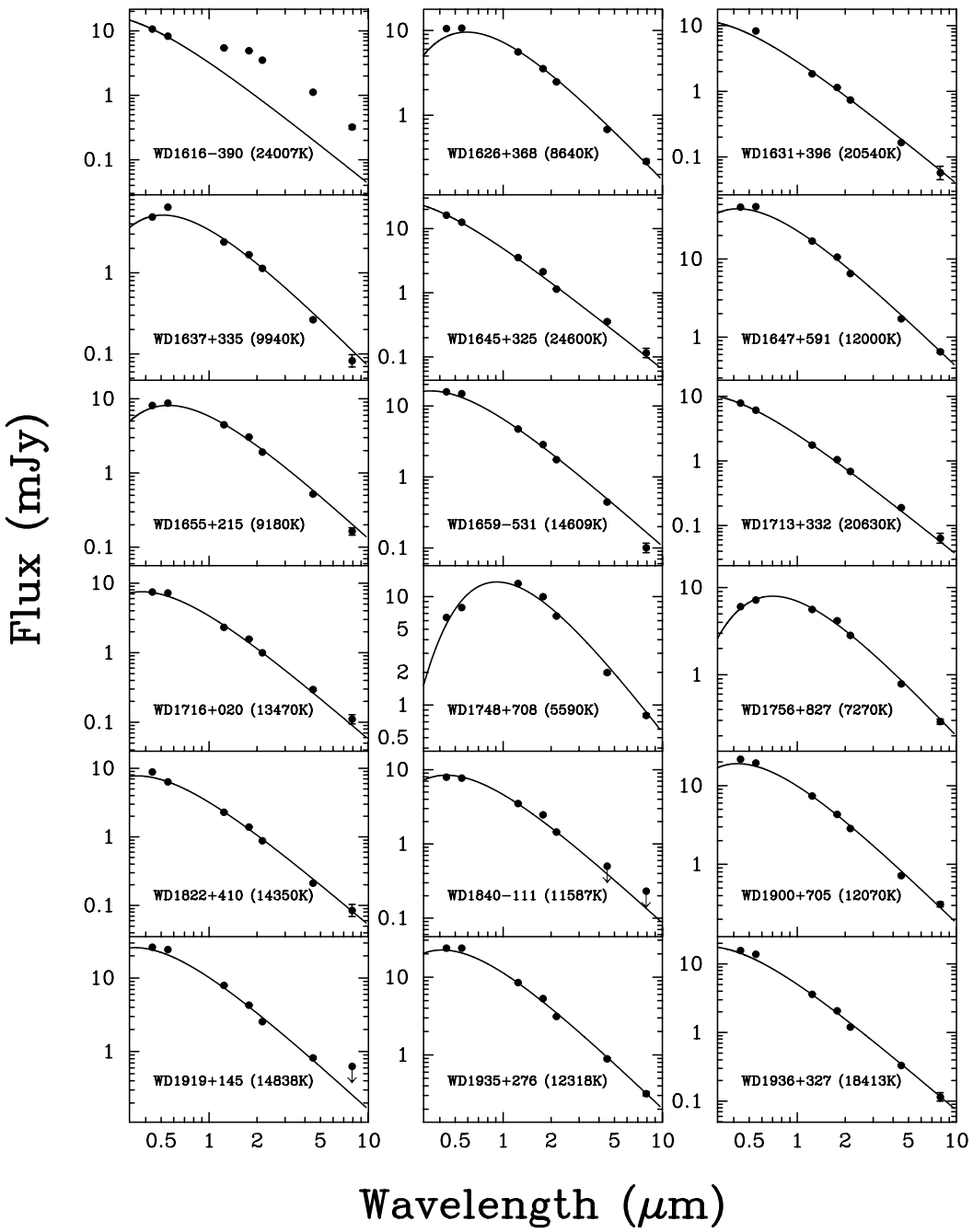

FIG. 1—*Continued*

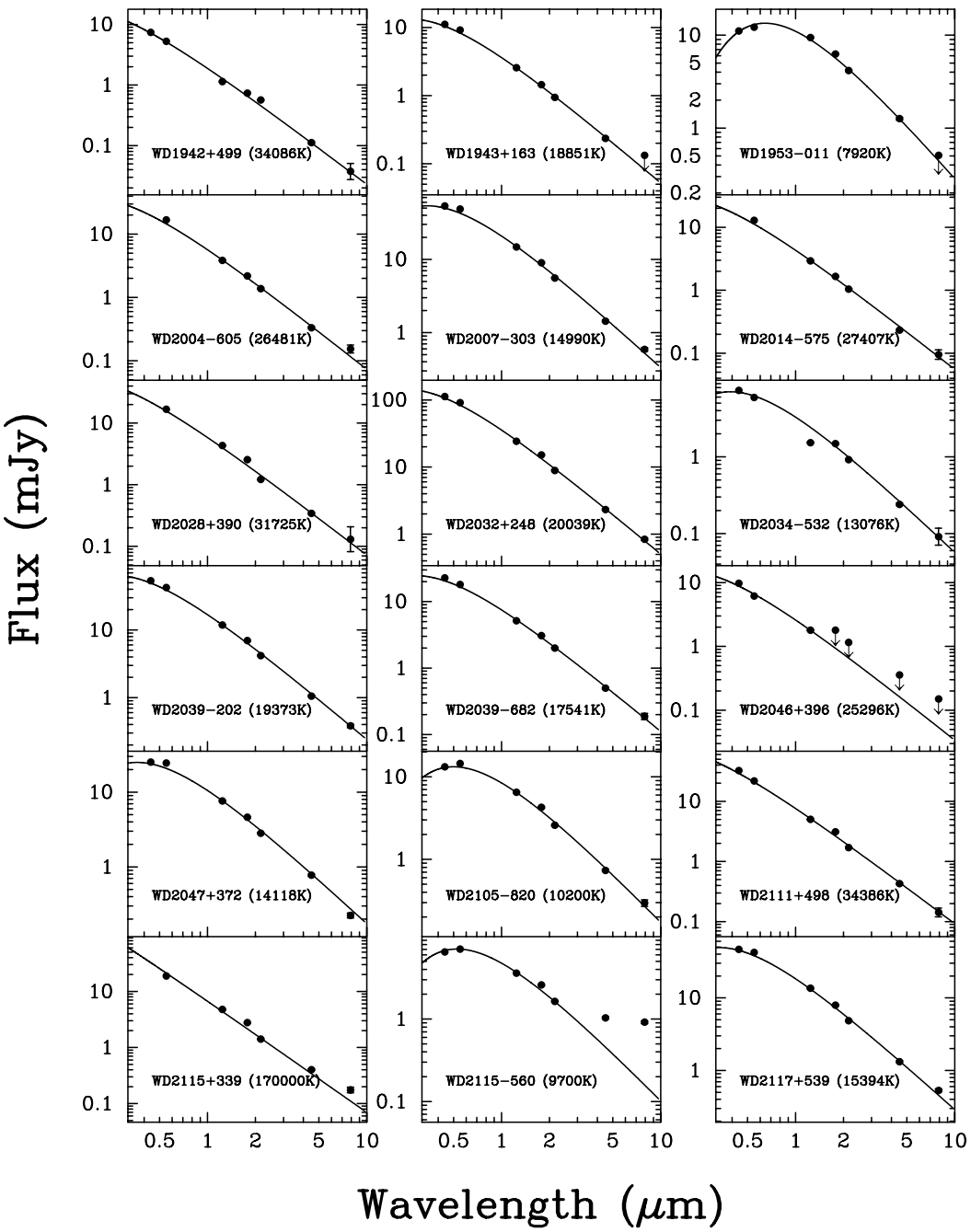

FIG. 1—*Continued*

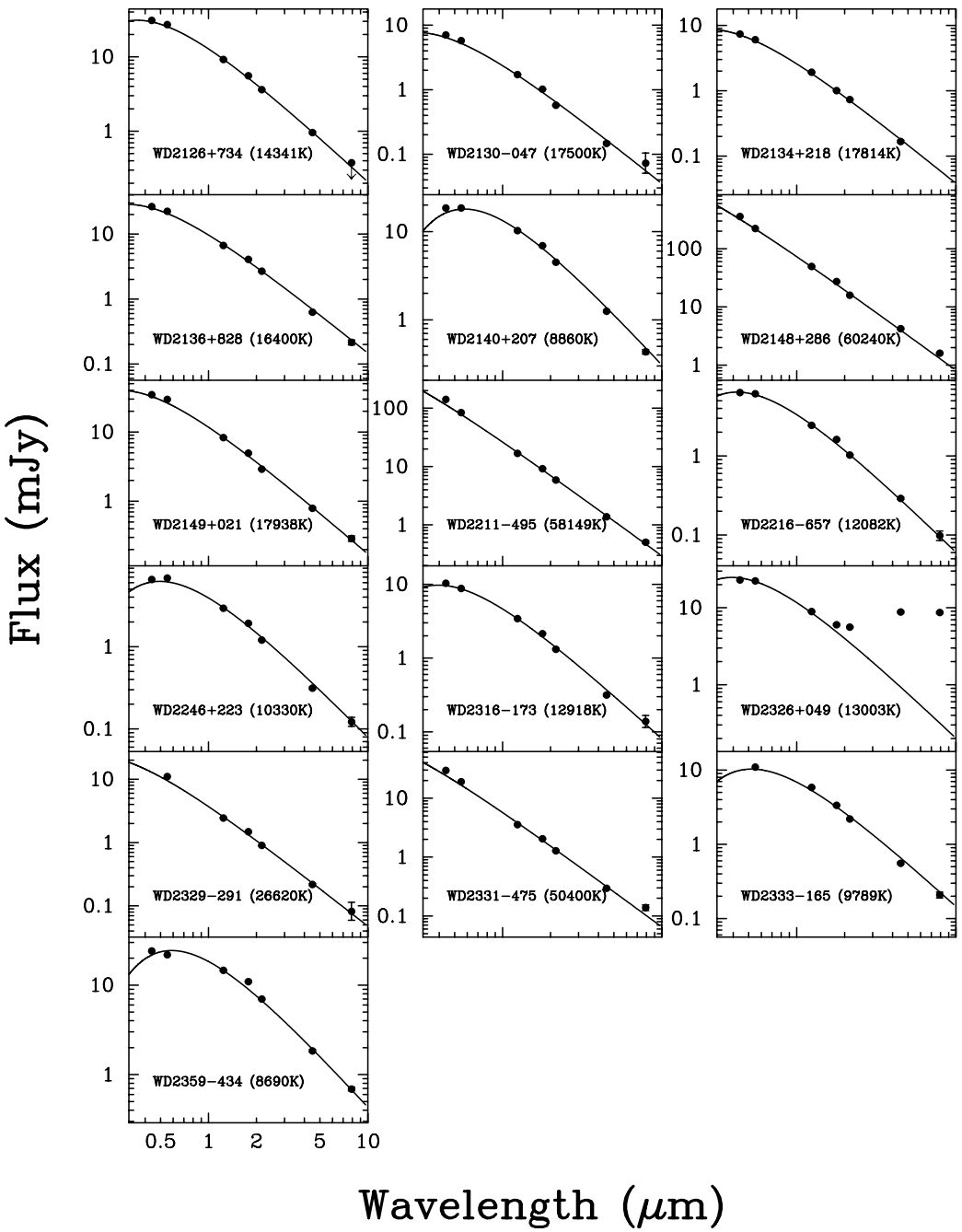

FIG. 1—*Continued*

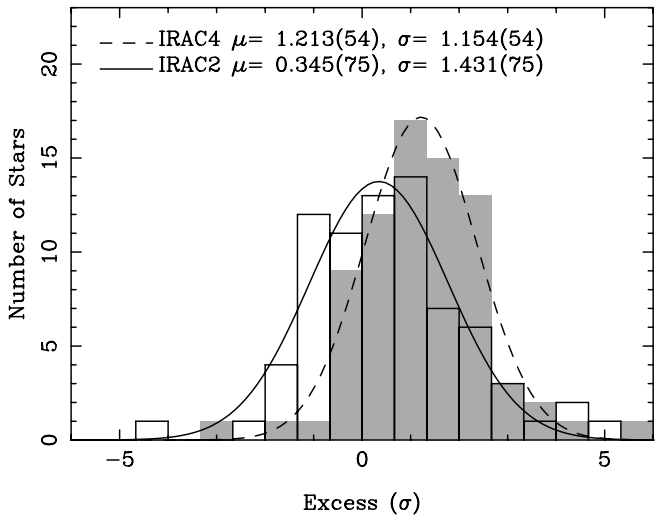

FIG. 2.—Histogram of excesses and deficits for a selection of the DAs observed in this survey. Each bin represents the difference between the observed flux and that predicted by models from Finley et al. (1997) as a fraction of the size of the measured photometric error. If no stars show unusual behavior, we expect this histogram to be well fit by a Gaussian with mean 0 and a standard deviation of 1. IRAC 2 is shown as white bars fit with the solid line, while IRAC 4 is shown as the gray histogram fit with the dashed line. The mean of each distribution is given by μ, while the standard deviation is given by σ. See text for discussion.

corresponds to IRAC channel 4 photometry, and the fitted Gaussian is plotted with a dashed line. The outlined histogram corresponds to channel 2, and the Gaussian is shown as a solid line. The dispersion in channel 2 is measurably greater than expected, indicating that our error bars may be underestimated. The measured flux in channel 4 is on average 1 σ higher than expected. This may be because the majority of stars have excess flux in this band (possibly due to a disk) or because of a poor match of our models to reality. As these models are well tested only in the optical regime for which they were originally intended, it is possible that this result points to new and unexpected physical processes affecting the mid-infrared portion of the spectrum.

Three brown dwarf companions to WDs are known (Becklin & Zuckerman 1988; Farihi & Christopher 2004; Maxted et al. 2006). In our survey we find one object with an SED consistent with a brown dwarf companion, or a detection frequency of $\lesssim$1%. The survey of Farihi et al. (2005) set the observed brown dwarf companion fraction at $0.4\% \pm 0.1\%$, consistent with our result. Our selection of targets deliberately excluded stars with known main-sequence binary companions, explaining the dearth of such companions in our sample. Both subdwarf stars in our survey show an infrared excess. This is consistent with the survey of Allard et al. (1994), who determined that 54%–66% of subdwarf stars have a main-sequence companion.

Table 3 lists the 20 objects in our survey with measured abundances of metal in their photospheres. Two of these objects (WD 2115 and WD 2326) have debris disks. HKK06 suggest that all DAZs are accreting from debris disks. The small fraction of DAZs with disks initially appears to refute this claim. It should be noted that for stars with temperatures $\gtrsim$19 kK, dust from any debris disk inside the Roche limit is expected to sublimate quickly and will not produce a noticeable infrared signature. For the cooler stars, the metal abundances are significantly lower and the flux from the debris disk is expected to be correspondingly dimmer.

TABLE 3
SURVEY OBJECTS WITH DETECTED PHOTOSPHERIC METALS

Name	[Ca/H]	$T_{\rm eff}$ (K)	Type	Reference
WD 0002+729	−11.4	13750	DBZ	1
WD 0005+511	...	47083	DO	2
WD 0455−282	...	57273	DA	2
WD 0501+527	...	40588	DA	2
WD 0552−041	...	5060	DZ	3
WD 0621−376	...	48333	DA	2
WD 0843+358	−9.6	17103	DBZ	1
WD 1202−232	−9.8	8567	DAZ	4
WD 1337+705	−6.7	20970	DAZ	4
WD 1626+368	−8.65	8640	DBZ	5
WD 1645+325	...	24600	DB	2
WD 1822+410	−8.15	14350	DZ	5
WD 2032+248	...	20039	DA	2
WD 2105−820	−8.6	10200	DAZ	6
WD 2111+498.....	...	34386	DA	2
WD 2115−560.....	−7.6	9700	DAZ	4
WD 2149+021	−7.7	17938	DAZ	4
WD 2216−657	−9.1	12082	DZ	6
WD 2326+049	−6.4	13003	DAZ	4
WD 2331−475	...	50400	DA	2

NOTE.—Objects with traces of metals in their photosphere in this survey.
REFERENCES.—(1) Dupuis et al. 1993; (2) Holberg et al. 2003; (3) Eggen & Greenstein 1965; (4) Koester & Wilken 2006; (5) Wolff et al. 2002; (6) Koester et al. 2005.

Deeper observations will be required to confirm or refute this hypothesis.

5. CONCLUSION

We have conducted a large mid-infrared white dwarf photometric survey, obtaining images of 124 WDs with a limiting sensitivity better than 0.1 mJy. This survey has already found an unexplained flux deficit in the SED of a cool white dwarf, and a debris disk around another star. This data set can be used to constrain the presence of planets around these stars, as well as to test and refine model white dwarf atmospheres.

This work is based on observations made with the *Spitzer Space Telescope*, which is operated by the Jet Propulsion Laboratory (JPL), California Institute of Technology, under NASA contract 1407. Support for this work was provided by NASA through award project NBR 1269551 issued by JPL/Caltech to the University of Texas. This work is performed in part under contract with JPL funded by NASA through the Michelson Fellowship Program. JPL is managed for NASA by the California Institute of Technology. This publication makes use of data products from the Two Micron All Sky Survey, which is a joint project of the University of Massachusetts and the Infrared Processing and Analysis Center/California Institute of Technology, funded by the National Aeronautics and Space Administration and the National Science Foundation. This research has also made use of the SIMBAD database, operated at CDS, Strasbourg, France

Facilities: Spitzer (IRAC)

REFERENCES

Allard, F., Wesemael, F., Fontaine, G., Bergeron, P., & Lamontagne, R. 1994, AJ, 107, 1565
Becklin, E. E., Farihi, J., Jura, M., Song, I., Weinberger, A. J., & Zuckerman, B. 2005, ApJ, 632, L119
Becklin, E. E., & Zuckerman, B. 1988, Nature, 336, 656
Bohlin, R. C., Dickinson, M. E., & Calzetti, D. 2001, AJ, 122, 2118
Burleigh, M. R., Clarke, F. J., & Hodgkin, S. T. 2002, MNRAS, 331, L41
Burrows, A., Sudarsky, D., & Lunine, J. I. 2003, ApJ, 596, 587
Chary, R., Zuckerman, B., & Becklin, E. E. 1998, in The Universe as Seen by *ISO*, ed. P. Cox & M. F. Kessler (ESA-SP 427; Noordwijk: ESA), 289
Chu, Y.-H., Dunne, B. C., Gruendl, R. A., & Brandner, W. 2001, ApJ, 546, L61
Debes, J. H., Ge, J., & Ftaclas, C. 2006, AJ, 131, 640
Debes, J. H., Sigurdsson, S., & Woodgate, B. E. 2005, AJ, 130, 1221
Dupuis, J., Fontaine, G., & Wesemael, F. 1993, ApJS, 87, 345
Eggen, O. J., & Greenstein, J. L. 1965, ApJ, 141, 83
Farihi, J., Becklin, E. E., & Zuckerman, B. 2005, ApJS, 161, 394
Farihi, J., & Christopher, M. 2004, AJ, 128, 1868
Fazio, G. G., et al. 2004, ApJS, 154, 10
Finley, D. S., Koester, D., & Basri, G. 1997, ApJ, 488, 375
Giovannini, O., Kepler, S. O., Kanaan, A., Wood, A., Claver, C. F., & Koester, D. 1998, Baltic Astron., 7, 131
Holberg, J. B., Barstow, M. A., & Burleigh, M. R. 2003, ApJS, 147, 145
Holberg, J. B., Barstow, M. A., & Sion, E. M. 1998, ApJS, 119, 207
Homeier, D., Koester, D., Hagen, H.-J., Jordan, S., Heber, U., Engels, D., Reimers, D., & Dreizler, S. 1998, A&A, 338, 563
Houck, J. R., et al. 2004, ApJS, 154, 18
Jura, M. 2003, ApJ, 584, L91
Kilic, M., von Hippel, T., Leggett, S. K., & Winget, D. E. 2005, ApJ, 632, L115
Kilic, M., von Hippel, T., Mullally, F., Reach, W. T., Kuchner, M. J., Winget, D. E., & Burrows, A. 2006, ApJ, 642, 1051
Kilkenny, D., Heber, U., & Drilling, J. S. 1988, S. African Astron. Obs. Circ., 12, 1
Koester, D., Rollenhagen, K., Napiwotzki, R., Voss, B., Christlieb, N., Homeier, D., & Reimers, D. 2005, A&A, 432, 1025
Koester, D., & Wilken, D. 2006, A&A, 453, 1051
Koester, D., et al. 2001, A&A, 378, 556
Kurucz, R. L. 1979, ApJS, 40, 1
Liebert, J., Bergeron, P., & Holberg, J. B. 2005, ApJS, 156, 47
Lisker, T., Heber, U., Napiwotzki, R., Christlieb, N., Han, Z., Homeier, D., & Reimers, D. 2005, A&A, 430, 223
Maxted, P. F. L., Marsh, T. R., & Moran, C. K. J. 2000, MNRAS, 319, 305
Maxted, P. F. L., Napiwotzki, R., Dobbie, P. D., & Burleigh, M. R. 2006, Nature, 442, 543
McCook, G. P., & Sion, E. M. 1999, ApJS, 121, 1
Oke, J. B. 1990, AJ, 99, 1621
Oke, J. B., Weidemann, V., & Koester, D. 1984, ApJ, 281, 276
Probst, R. G. 1983, ApJS, 53, 335
Reach, W. T., Kuchner, M. J., von Hippel, T., Burrows, A., Mullally, F., Kilic, M., & Winget, D. E. 2005a, ApJ, 635, L161
Reach, W. T., et al. 2005b, PASP, 117, 978
Sion, E. M., Fritz, M. L., McMullin, J. P., & Lallo, M. D. 1988, AJ, 96, 251
Skrutskie, M. F., et al. 2006, AJ, 131, 1163
Sudarsky, D., Burrows, A., & Hubeny, I. 2003, ApJ, 588, 1121
Thejll, P., MacDonald, J., & Saffer, R. 1991, A&A, 248, 448
Tremblay, P.-E., & Bergeron, P. 2007, ApJ, in press (astro-ph/0611899)
Wegner, G., & Swanson, S. R. 1990, AJ, 99, 330
Weidemann, V. 2000, A&A, 363, 647
Werner, K., Dreizler, S., Heber, U., Rauch, T., Fleming, T. A., Sion, E. M., & Vauclair, G. 1996, A&A, 307, 860
Werner, M. W., et al. 2004, ApJS, 154, 1
Wickramasinghe, N. C., Hoyle, F., & Al-Mufti, S. 1988, Ap&SS, 143, 193
Wolff, B., Koester, D., & Liebert, J. 2002, A&A, 385, 995
Zuckerman, B., & Becklin, E. E. 1987, Nature, 330, 138
———. 1992, ApJ, 386, 260
Zuckerman, B., Koester, D., Reid, I. N., & Hünsch, M. 2003, ApJ, 596, 477